Test of shower reconstruction procedures with the IceTopA, IceTopB subarrays

J. Ochab*

12.09.2007

Abstract

Using the IceTop array divided into two equivalent subarrays a test of shower core, direction and size reconstruction was done. Estimated resolution of core position using lateral fit amounts to $14.14 \pm 0.30\,\mathrm{m}$, the combined fit's angular resolution is $1.230 \pm 0.014°$. The choice of S_{125} was suggested as the fitting parameter of the lateral distribution function, although S_{100} is still a valid one. Fluctuations of reconstructed S_R values were found to have decreased significantly since last examinations. Observations on tank response threshold effects as well as on R_{trans} dependence upon shower size were made.

1 Introduction

The IceTop detector array comprises stations of two equivalent 10m distant tanks. Thus, it can be divided into two subarrays, named IceTopA and IceTopB, characterised by almost identical spacing and size as the complete one. Nevertheless, shower fluctuations as well as tank response fluctuations occur, which is reflected in differences between A and B measurements. A comparison of shower reconstructions made with the data collected by either array can provide an estimate of the IceTop resolution.

1.1 Data used

The data used in the analysis is measurements from 16.10.2006 made by 16 operating stations, which contains 22435 air showers overall.

1.2 Cuts applied

In order to discard unreliably reconstructed events several cuts have been applied. Most commonly used 'CutN' means that N stations were required to be hit (the minimum N being 5, so that fitting procedure could take place). 'ContainedM' cut denotes events whose reconstructed cores lie within the area of the array with boundaries shrinked by M metres from all sides. 'CutN+' is CutN and Contained50 cuts combined. The only exception is constantly used 'Cut5+', which among other includes also cuts on β parameter and zenith angle θ.

The variety of cuts is mostly due to comparison with the previous report's results [1]. Each time when it is necessary to know which cuts were applied they are mentioned.

2 Shower core reconstructions

2.1 Methods

The error calculus on the core position error is based on the assumption that the values of x and y coordinates of reconstructed core positions fluctuate randomly with a normal distribution. Its standard deviations $\sigma_{x,y}$ are the same for x and y.

*ochab@corcoran.if.uj.edu.pl

Standard deviation of $|\Delta\vec{x}| = |\vec{x_A} - \vec{x_B}| = \sqrt{(x_A - x_B)^2 + (y_A - y_B)^2}$ is then given by

$$\sigma_{A-B} = \sqrt{\left(\sigma_{x,y} \cdot \frac{x_A - x_B}{|\Delta\vec{x}|}\right)^2 + \left(\sigma_{x,y} \cdot \frac{y_A - y_B}{|\Delta\vec{x}|}\right)^2} = \sqrt{2}\sigma_{x,y} \quad . \tag{1}$$

The complete array delivers proximately the mean of both subarrays, therefore the standard deviation for each coordinate is given by

$$\sigma_m = \sigma_{x,y}/\sqrt{2} = \sigma_{A-B}/2 \quad , \tag{2}$$

where the quantity obtained from the data is σ_{A-B}.

The value σ_{A-B} was calculated in two ways: either as the peak of $|\Delta\vec{x}|$ distribution or as the value for which 68% of the distribution's integral is reached (to disambiguate between those two σ_m and $\sigma_{m,68\%}$ are used respectively).

In the former case Moyal's distribution was used to parametrise the distribution:

$$f(x) = c \cdot \exp\left[-\frac{1}{2}\left(\frac{x-p}{\sigma} + \exp\left(-\frac{x-p}{\sigma}\right)\right)\right] \quad , \tag{3}$$

where c, p, σ are fitting parameters and p gives the peak position. Moyal's distribution proved to fit the data better than theoretically derived one:

$$g(x) = c \cdot x \cdot \exp\left(-\frac{x^2}{2\sigma^2}\right) \quad .$$

The error given is the curve fitting error of the p parameter. This way was chosen for the sake of comparison with the previous results.

In the case of 68% integral calculation, the data was was divided into four even samples, integrals were computed directly using finest binning and mean was taken. The error given is the standard deviation estimator

$$S\{\bar{x}\} = \sqrt{\frac{1}{n \cdot (n-1)} \sum_{i=1}^{n} (x_i - \bar{x})^2} \quad . \tag{4}$$

2.2 Results

To determine σ_m values for both centre of gravity (COG) and lateral fit Cut8 was used. Additionally the position of the reconstructed core had to lay within the boundaries of the array (Contained0) and some less dominant cuts on β parameter and θ angle were applied. Those limitations very closely reproduced the cuts used formerly [1]. One can see in Fig.1 $|\Delta\vec{x}|$ distributions for COG and lateral fits, as well as fitted Moyal's distributions and the obtained peak positions. The numerical results are as follows (the errors indicated are merely fitting errors):

$$\begin{aligned} \sigma_{m,\mathrm{COG}} &= 6.114 \pm 0.085\,\mathrm{m} \\ \sigma_{m,\mathrm{LAT}} &= 6.32 \quad \pm 0.13\,\mathrm{m} \quad , \end{aligned} \tag{5}$$

whereas the previously obtained values [1] are:

$$\begin{aligned} \sigma_{m,\mathrm{COG}} &= 5.4\,\mathrm{m} \\ \sigma_{m,\mathrm{LAT}} &= 8.4\,\mathrm{m} \quad . \end{aligned}$$

In the 68%-method the newly introduced Cut5+ was applied (as described in Section 1.2). The results are illustrated in Figure 2 and numbers given below (errors being standard deviation estimator, as mentioned above):

$$\begin{aligned} \sigma_{m,\mathrm{COG},68\%} &= 11.57 \pm 0.10\,\mathrm{m} \\ \sigma_{m,\mathrm{LAT},68\%} &= 14.14 \pm 0.30\,\mathrm{m} \quad . \end{aligned} \tag{6}$$

Additionally Figures 3a,b show a comparison between fluctuations of core position in x and y directions. $\sigma_{A-B,68\%}$ deviations were calculated using the 68% method as above (only the mean was not taken, as σ_m is not of particular interest here) and Cut5+ was imposed. The results are given below, for COG:

$$\begin{aligned}\sigma_{A-B,\mathrm{X},68\%} &= 14.74 \pm 0.28\,\mathrm{m}\\ \sigma_{A-B,\mathrm{Y},68\%} &= 15.07 \pm 0.10\,\mathrm{m} \quad ,\end{aligned} \tag{7}$$

and for lateral fit:

$$\begin{aligned}\sigma_{A-B,\mathrm{X},68\%} &= 17.90 \pm 0.38\,\mathrm{m}\\ \sigma_{A-B,\mathrm{Y},68\%} &= 17.81 \pm 0.36\,\mathrm{m} \quad .\end{aligned} \tag{8}$$

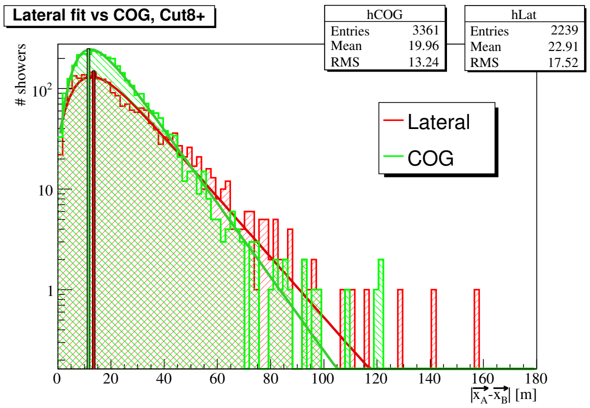

Figure 1: Comparison of fluctuations of reconstructed core position for lateral fit and COG. Fitted Moyal's distribution function and obtained peak positions σ_m are indicated.

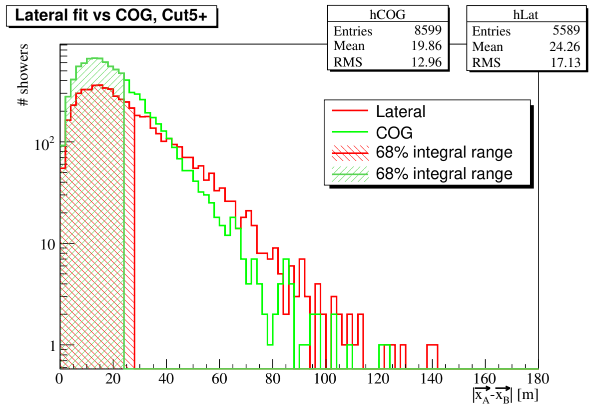

Figure 2: Comparison of fluctuations of reconstructed core position for lateral fit and COG. The $\sigma_{m,68\%}$ values (68% integral ranges) are indicated.

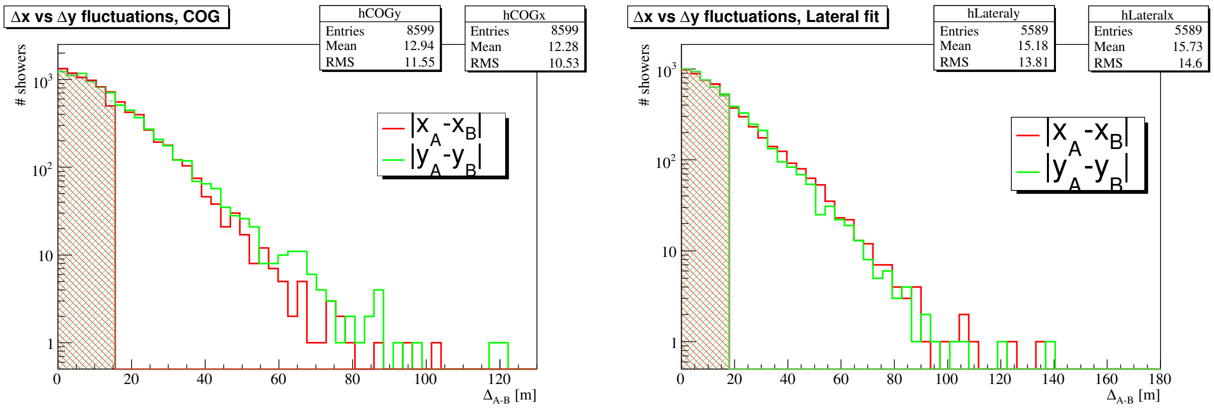

(a) (b)

Figure 3: Comparison between fluctuations of reconstructed core position in x and y coordinates for both (a) COG and (b) lateral fit. The shaded area corresponds to 68% of events.

2.3 Discussion

One should bear in mind that the determined σ_m, $\sigma_{m,68\%}$ values describe only the fluctuations of reconstructed core position. They do not provide us easily with the distance of reconstructed core position from the true core position, so we can't determine the error of the core position (this is possible only by studying simulations). What we get is the extent to which two subarrays' reconstructions are consistent, i.e. the stability of the fitting method. At the same time these values determine the maximal resolution of reconstruction procedure.

Both σ_m and $\sigma_{m,68\%}$ values are smaller for the centre of gravity than for the lateral fit. Yet, the lateral fitting procedure has improved since the last study (for COG, σ_m should stay roughly unchanged and this is the case here). Those results mean that COG has remained the stabler procedure, although we know that it produces incorrect results (e.g. because it can reconstruct only core within the array area). Still the significance or interpretation of σ_m obtained from the peak position of the distributon seems rather vague. That is the reason why $\sigma_{m,68\%}$ was introduced: it gives certain quantitive information on 1σ-band width.

There is no significant asymmetry between x and y coordinates. Although there are differences to be seen in Fig.3, they are mostly visible above the $\sigma_{A-B,\mathrm{X,Y},68\%}$ value, so the fluctuations there are not prominent. Additionally $\sigma_{A-B,\mathrm{X},68\%}$ and $\sigma_{A-B,\mathrm{Y},68\%}$ do not differ for the lateral fit more than standard deviations allow. The situation is a little worse for COG, but still it may have additional uncertainties due to flaws of the method.

3 Shower front reconstructions

3.1 Methods

Calculations from the previous paragraph hold for the angular resolution of shower front direction reconstruction. Thus $\sigma_m = \sigma_{A-B}/2$, where σ_m corresponds to the zenith and azimuth angles, while σ_{A-B} to the opening angle δ_{A-B}. The formula for the opening angle is given by:

$$\begin{aligned}\delta_{A-B} = 180/\pi \cdot \arccos \Big[&\frac{1}{2}\cos\left(\theta_A - \theta_B\right) \cdot \Big(1 + \cos\left(\phi_A - \phi_B\right)\Big) \\ &+\frac{1}{2}\cos\left(\theta_A + \theta_B\right) \cdot \Big(1 - \cos\left(\phi_A - \phi_B\right)\Big)\Big] \quad .\end{aligned}$$

where $\theta_{A,B}, \phi_{A,B}$ are zenith and azimuth angle respectively. Methods of determining σ_{A-B} values remain identical with those given in Sec.2.1.

3.2 Results

Cuts applied to the data used in analysis of shower front reconstruction are in principle the same as in Section 2.2. The only difference is that cuts were applied to values from combined or plane fit (depending on which fit one want to scrutinise and what values can particular fit produce), e.g. Combined0 or Contained50 cuts correspond here to core positions calculated with combined fit.

In comparison with the formerly produced results it is relevant to remember, that 'plane fit' uses plane shower front model, while 'combined fit' makes use of a curved shower front. Values taken from [1] are labeled with respect to the shower front model, as before there was no 'combined fit' procedure.

The results for the peak position method are (once again, fitting errors are given for the peak position parameter):

$$\begin{aligned}\sigma_{m,\mathrm{PLANE}} =& 0.781 \pm 0.012^\circ \\ \sigma_{m,\mathrm{COMB}} =& 0.56 \ \ \pm 0.01^\circ \quad ,\end{aligned} \tag{9}$$

while the previously obtained values[1] are:

$$\begin{aligned}\sigma_{m,\mathrm{PLANE}} &= 0.82^\circ \\ \sigma_{m,\mathrm{CURVED}} &= 0.81^\circ \quad .\end{aligned}$$

The results for the 68% of distribution integral method are (errors being standard deviation estimator for four measurements):

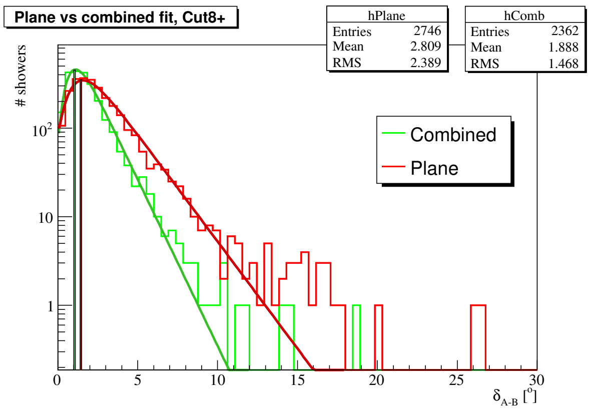

Figure 4: Comparison of fluctuations of reconstructed shower front direction for plane and combined fits. Fitted Moyal's distribution function and obtained peak positions are indicated.

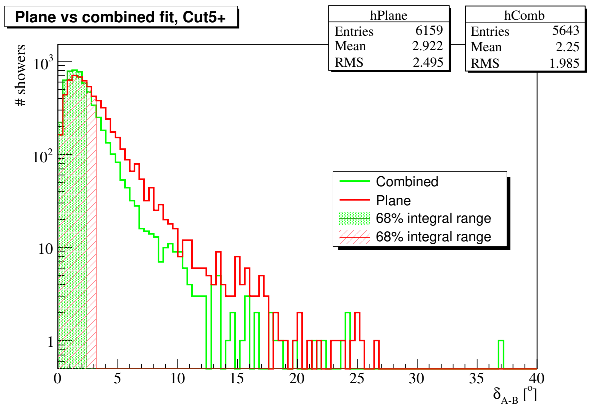

Figure 5: Comparison of fluctuations of reconstructed shower front direction for plane and combined fits. The $\sigma_{m,68\%}$ values (68% integral ranges) are indicated.

$$\begin{aligned} \sigma_{m,\mathrm{PLANE},68\%} &= 1.606 \pm 0.017^\circ \\ \sigma_{m,\mathrm{COMB},68\%} &= 1.230 \pm 0.014^\circ \quad . \end{aligned} \tag{10}$$

Corresponding figures are Figure 4 for the former method and Figure 5 the latter one, respectively.

3.3 Discussion

The new fitting procedure, that is the combined fit, proves to be a stabler method than mere plane fit (both σ_m and $\sigma_{m,68\%}$ are smaller for the combined fit, as well as the distribution of fluctuations is more centralised around zero). In Fig.5 there is 500 less events for the combined than for the plane fit, but the difference does not change shapes of the distributions (it was checked simply by decreasing the sample for the plane fit histogram, to obtain the same number of events). At the same time, there are no considerable differences between previous and present plane fit results.

4 S_R reconstructions

4.1 S_R fluctuations in general

In Figure 6 distribution of $\log_{10}(S_A/S_B)$ (i.e. of $\log_{10}(S_R)$ fluctuations) is plotted. For the sake of comparison Cut8 and Contained0 was used, NKG was the fitting function with S_{100} as a parameter and only lateral fit results were taken into account. The width of these distributions have changed prominently since results presented in [1]: peaks are two times narrower than before (in $\log_{10}$ units). Although the plots presented here have three times less events included, clearly that does not influence the resulting width as much.

In Fig.7 fluctuations of S_{100}, $S_{R_{trans}}$ and reconstructed energy are compared. $S_{R_{trans}}$ is the value used for shower energy extraction. R_{trans} is discussed later on in Sec.5. One can see, that the distribution of $S_{R_{trans}}$ is a little narrower, which makes it a better quantity to extract energies.

Figure 8 gives a comparison of S_R fluctuations for various fitting functions. Here the most recent Cut5+ was imposed on the data and reconstruction results were obtained using combined fit (there is no need to refer to previous results and the Cut5+ provides us with higher statistics and more reliable data, while combined fit proved to be the stablest procedure in Sec. 2 and 3). The widths do not differ significantly, especially for the 125m (0.5-1.5%) and 100m (5-11%), which is to be seen also in Fig.9.

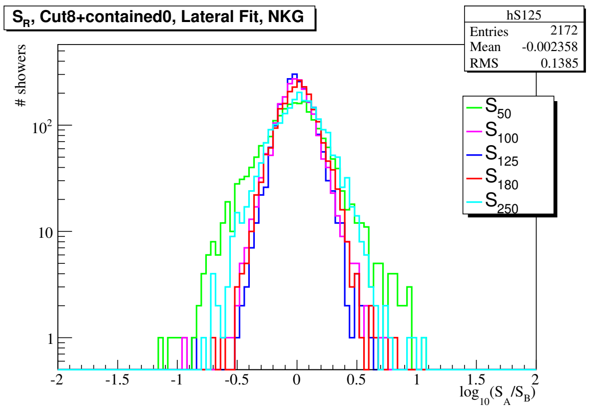

Figure 6: Distribution of signal S_R fluctuations for several radii. Cuts most similar to that in [1] were used.

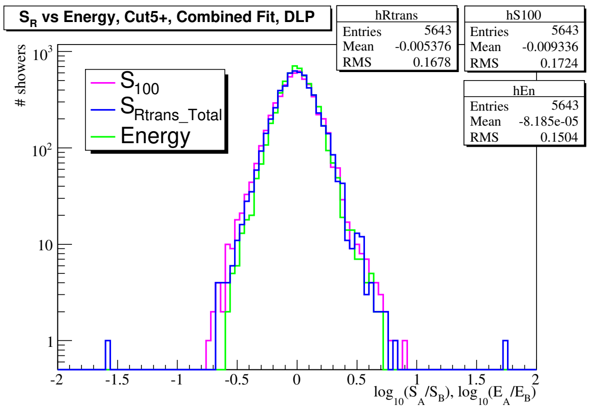

Figure 7: A comparison of S_{100}, $S_{R_{trans}}$ and reconstructed energy fluctuations. $S_{R_{trans}}$ is used to extract shower energies.

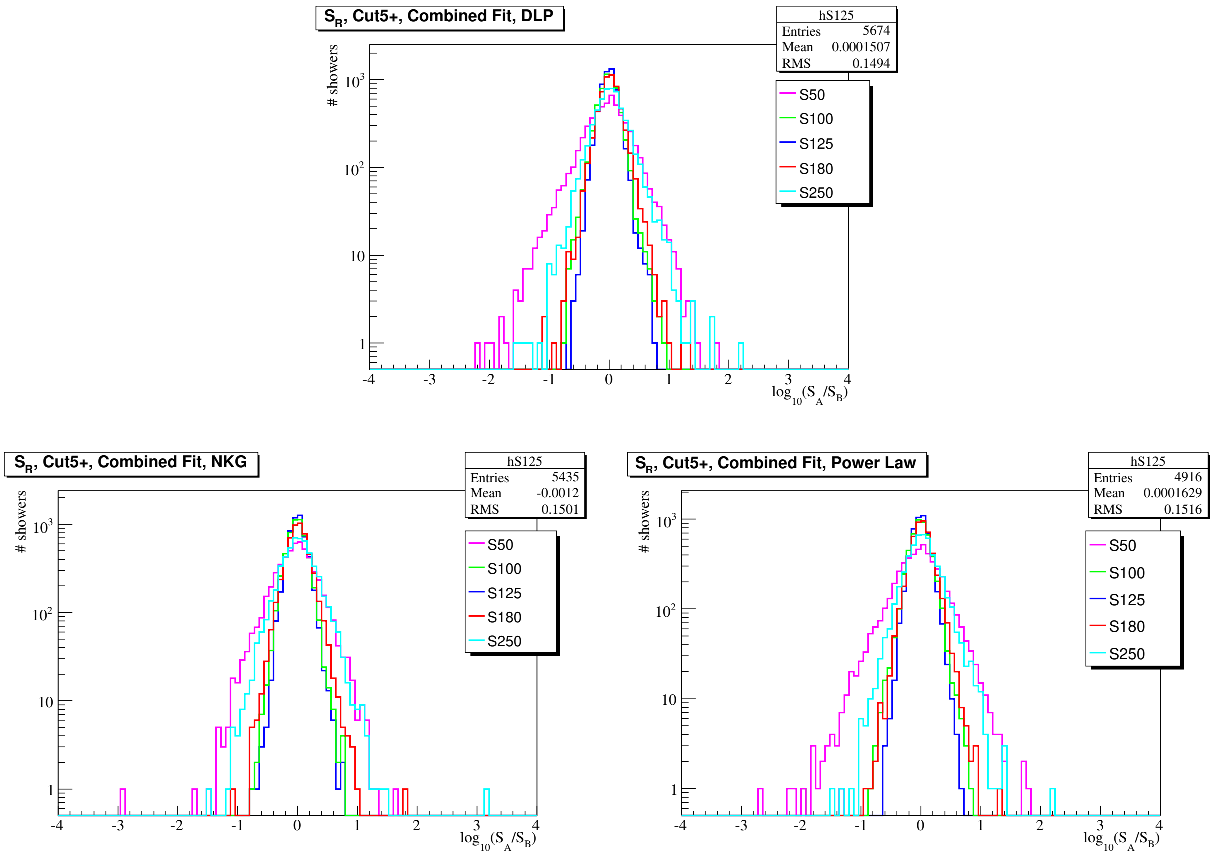

Figure 8: Distribution of signal S_R fluctuations for several radii. Results for DLP, NKG and power law are compared. Cut5+ was applied to the data and reconstructions used combined fit.

4.2 S_R fluctuations' minimum

One of the arguments for the choice of S_{100} as the fitting parameter was its smaller fluctuations compared with the other S_R. In Fig.9 the behaviour of RMS values of S_R fluctuations are shown (this can also be seen in figure 8 as the widths of the plotted distributions). In those calculations Cut5+ was applied (without cuts on β, because the parameter has different meaning in DLP and NKG functions, and is absent in power law) and combined fitting of either DLP, NKG function or power law and the shower front curvature was used. An obvious minimum can be seen for the distance from a shower core around 125-135 m. When additional conditions on shower size (in the sense of number of stations hit) are applied, one observes that the curve become flatter especially at greater distances. As a result the minimum is slightly shifted and less distinct.

In conclusion, although S_{125} would be a stabler parameter, S_{100} still seems to be a valid choice. There is not a big difference between those two, when one deals with larger showers. For small showers the minimum is very distinct, but S_{100} value stays in a fairly flat region around it.

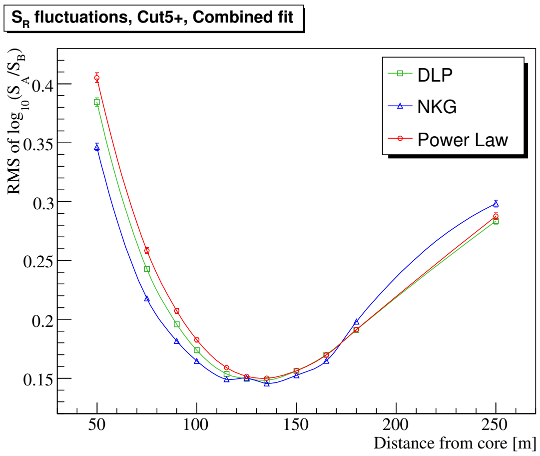

Figure 9: Dependence of S_R fluctuations on distance from the core R with minimum around 130 m. The curve to be seen is just an interpolation. DLP, NKG and power law are compared.

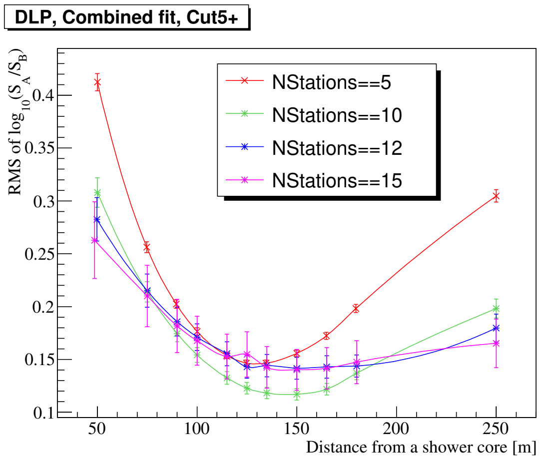

Figure 10: Dependence of S_R fluctuations on distance from the core R for various shower size (number of stations hit).

4.3 Additional checks

To check if the RMS values of $\log_{10}(S_A/S_B)$ and $\beta_A - \beta_B$ are reasonable a comparison with the fitting errors was carried out. Figures 12 and 14 give directly the RMS values. To calculate those using fitting errors we used the formula:

$$\sigma_{A,B} = \sqrt{\frac{1}{n}\sum_{i=0}^{n}\sigma_i^2} \quad , \tag{11}$$

where $\sigma_{A,B}$ stands for the RMS value of A or B subarray, σ_i is a fitting error for a given event and n is number of events (that is illustrated by figures 11 and 13). Then:

$$\sigma_\beta = \sqrt{\sigma_A^2 + \sigma_B^2} \quad . \tag{12}$$

As only S_{100} errors are given, directly one has to calculate first

$$\sigma_{\log_{10}(S_{100,A})} = \sigma_{S_{100,A}}/(\ln 10 \cdot S_{100,A}) \tag{13}$$

for A or B subarrays and next do the same thing as for σ_β.

Below 'RMS' denotes values obtained from figures 12 and 14, while 'σ' give results of calculations described above:

$$\begin{aligned} \sigma_{\log_{10}(S_{100,A})} &= 0.15 \\ RMS\left(\log_{10}\left(S_{100,A}/S_{100,B}\right)\right) &= 0.17 \end{aligned} \tag{14}$$

$$\begin{aligned} \sigma_{\beta} &= 0.82 \\ RMS\left(\beta_B - \beta_A\right) &= 0.78 \quad . \end{aligned} \tag{15}$$

In these calculations, both for $\log_{10}(S_{100})$ and β, range of β fitting error ($\Delta\beta$) was restricted to the interval $[0, 3.76]$, to be in agreement with Cut5+, which includes the cut: $1 < \beta < 6.5$ (hence $\Delta\beta \leq 5.5 * 68.27\% \approx 3.76$ was taken, if one treats $[0, 5.5]$ interval as the maximum error). This cut deals well with events having undesirably large $\Delta \log_{10}(S_{100})$ values, as can be seen in Fig.13. Indeed, it should be suggested to include this kind of cut as a standard one in the IceTop data analysis. Still, its proper definition needs to discussed.

The obtained results for $\log_{10}(S_{100})$, as well as for β match reasonably well with each other.

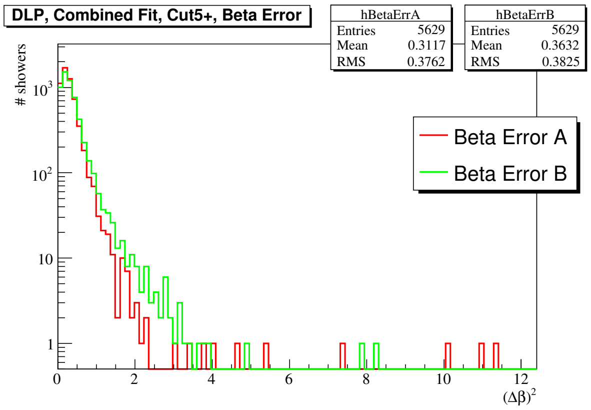

Figure 11: Squared β fitting error.

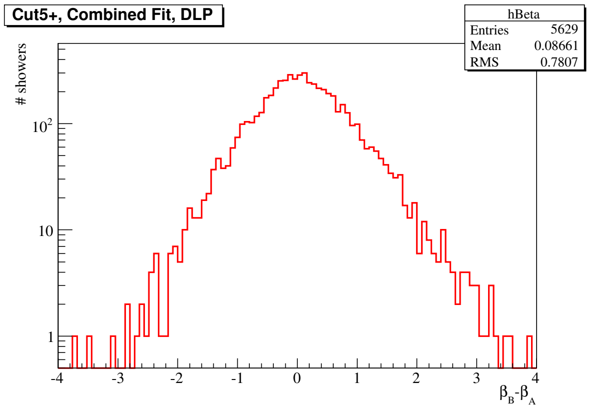

Figure 12: β fluctuations with the use of A and B array information.

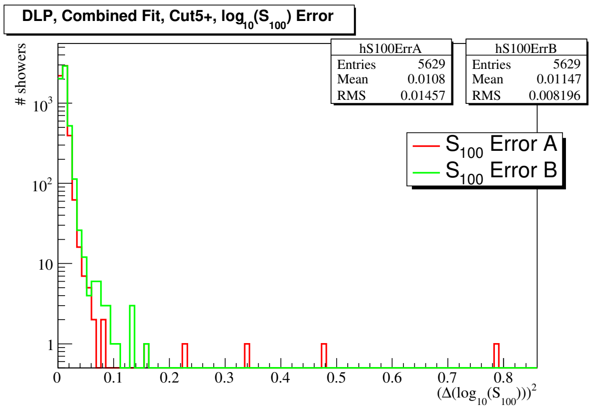

Figure 13: Squared $\log_{10}(S_{100})$ error obtained from S_{100} fitting error.

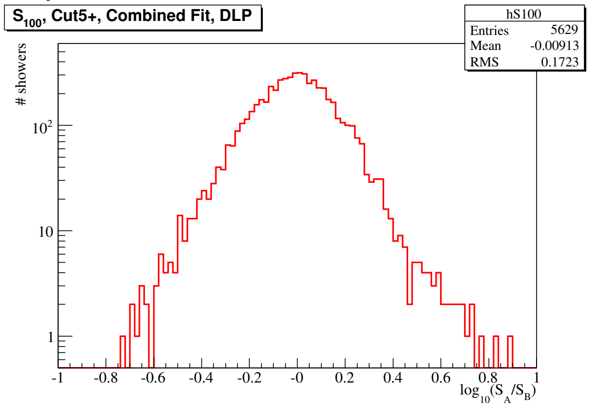

Figure 14: $\log_{10}(S_{100})$ fluctuations with the use of A and B array information.

4.4 $\log_{10}(S_A/S_B)$ mean value shift

A shift of $\log_{10}(S_A/S_B)$ mean value from zero has been observed. In Fig.15 the green line shows dependence of this shift on distance from a shower core. It should be reminded that the function used in the fitting procedure is a double logarithmic parabola [2]:

$$S(R) = S_{R_0} \left(\frac{R}{R_0}\right)^{-\beta-\kappa\,\log_{10}(R/R_0)} \tag{16}$$

where R is the distance from a shower core, β and S_{R_0} (for a fixed R_0 value, here 100m) are fitting parameters, and $\kappa = 0.303$. The supposition is that β parameter is responsible for the $\log_{10}(S_A/S_B)$ MV shift. Following the Eq.16:

$$\log_{10}(S_A/S_B) = (\beta_B - \beta_A) \cdot \log_{10}(R/100) \quad . \tag{17}$$

Then, e.g. using the information given in Fig.12, one can calculate the MV shift of $\log_{10}(S_A/S_B)$ resulting from MV shift of β parameter error. That is depicted as a red graph in Fig.15. The errors indicated there are given by:

$$\sigma_{(\log_{10}(S_A/S_B))} = \mathrm{RMS}\,(\beta_B - \beta_A) \cdot \log_{10}(R/100) \quad , \tag{18}$$

as one would usually calculate error propagation (R variable is exact here). The errors of directly calculated $\log_{10}(S_A/S_B)$ are RMS values of the distributions divided by square root of number of entries. The shapes of the two curves correspond to each other very well.

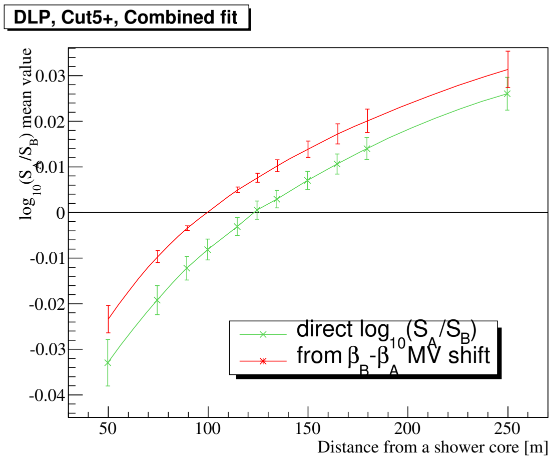

Figure 15: Green points give $\log_{10}(S_A/S_B)$ mean value shifts, e.g. as taken from Fig.8. Red points give values obtained from Eq.17. Curves plotted are interpolations.

Although we have got the simple explanation for $\log_{10}(S_A/S_B)$ MV shift, it appears that the shift is significant. Given number of entries, mean value and RMS of β error distribution in Fig.12:

$$\begin{aligned} \text{Entries} &= 5629 \\ \text{Mean} &= 0.08661 \\ \text{RMS} &= 0.7807 \end{aligned} \tag{19}$$

the standard deviation of all measurements is:

$$\sigma_\beta = \mathrm{RMS}/\sqrt{\text{Entries}} = 0.01041 \quad . \tag{20}$$

The shift of mean value is certainly too large and, unless one can trace where it comes from, it should be included in the systematic error of β.

5 R_{trans} behaviour

5.1 Introduction

A distinction between the reference radius R_{ref} of the fit function and the energy *transformation radius* R_{trans} was introduced by [3]:

While R_{ref} will later be fixed to a value that ensures that S_{ref} is as uncorrelated as possible to β, R_{trans} will be the radius whose $S(R_{trans}) = S_{trans}$ is the ideal quantity to extract energy from. Take notice that the two do not need to be equal, and in general neither of the two has to be a fixed value for all showers.

A method of choosing R_{trans} that turned out to deliver stable results is to take the radius that has the lowest fit uncertainty. In a power law fit like that of the lateral distribution function, this can be approximated by:

$$\log_{10} R_{trans} = \frac{1}{N}\sum_{i=1}^{N} \log_{10} R_i \qquad , \tag{21}$$

which has the advantage that it is an easy quantity to be calculated shower by shower and its use leads to a more homogeneous resolution function of the shower size.

5.2 Results

The data used included information from the whole array (hence 'Total' label in the plots), was restricted by Cut5+ and was processed with combined fit. Then, for consecutive numbers of stations hit by air showers R_{trans} values were obtained. 5 stations requirement was the minimum for the data to be fitted on one hand, 16 being the maximum number of operating stations on the other. The maximum was decreased to 15 due to very little recorded events. Figure 16 give overview of R_{trans} distribution for several 'NStations' cuts. For each of them the mean value and RMS was calculated. The results are depicted in the Fig.17. The fitted curve is given by the formula $R_{trans} = a \cdot \sqrt{N-b} + c$. Obviously, $N \sim R^2_{trans}$, as the number of stations corresponds to the area encircled by a shower. The fitted parameters' values are:

$$\begin{aligned} a =& 40.2 \pm 2.6\mathrm{m}/\sqrt{\mathrm{stations}} \\ b =& 0.11 \pm 0.94\mathrm{stations} \\ c =& 1 \pm 14\mathrm{m} \end{aligned} \tag{22}$$

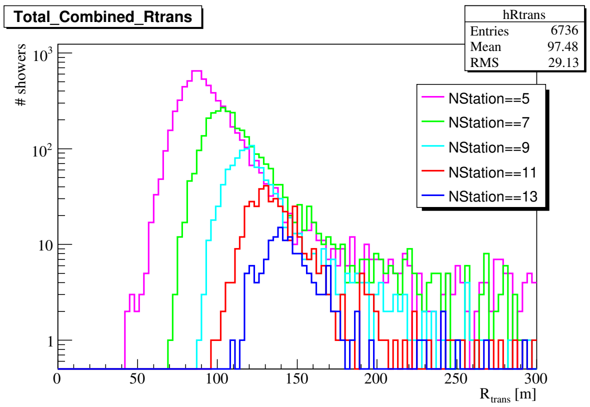

Figure 16: Distributions of R_{trans} values for various numbers of stations hit. The statistics given correspond to the 5 stations hit condition.

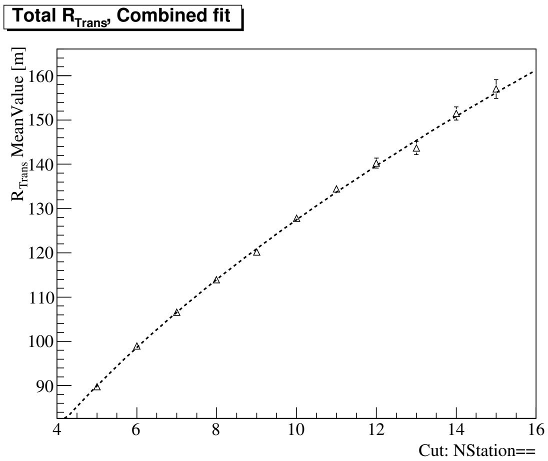

Figure 17: Mean value of R_{trans} taken from Fig.16 vs required number of stations hit. The fitted curve is given by: $R_{trans} = a \cdot \sqrt{N-b} + c$, where a, b, c are parameters, N is number of stations.

6 Stations' response

A few observations on threshold effects in stations' response were made. Those are illustrated by Figures 18a,b and 19. Due to the detection threshold small signals are missing from the data. In consequence the ratio S_{signal}/S_{fit} (where S_{signal} is the charge of pulses seen by detectors, and S_{fit} is the reconstructed signal) increases at large distances from a shower core, where only minute signals remain. That is shown in Fig.18a for 100m and 180m distances from a shower core.

The distribution of $\log_{10}(S_{signal}/S_{fit})$ have different shapes, depending on the distribution of distances between reconstructed shower core and a given station. Thus it is possible to distinguish between stations positioned in the corner, on the edge or inside the array. Fig.18b illustrates distributions for station 39, which is inside the array and there is a lot of reconstructed shower cores in its vicinity, and station 59, which is located at the border of the array and detects less nearby events.

The effect from Fig.18a plotted vs strength of the signal is additionally shown in the Fig.19. While strong signals have the same values for detected S_{signal} and reconstructed S_{fit} ($\log_{10}(S_{signal}/S_{fit})$ values fluctuate around zero), the small ones (on the left) are ignored by detectors, so that the ratio S_{signal}/S_{fit} increases. In fact, it is good to observe this behaviour, as it means that S_R values are reconstructed correctly.

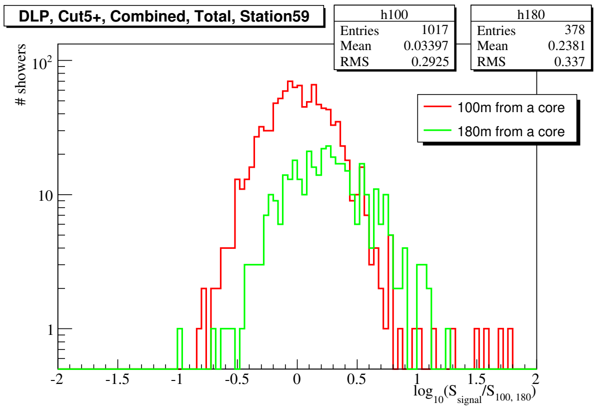

(a)

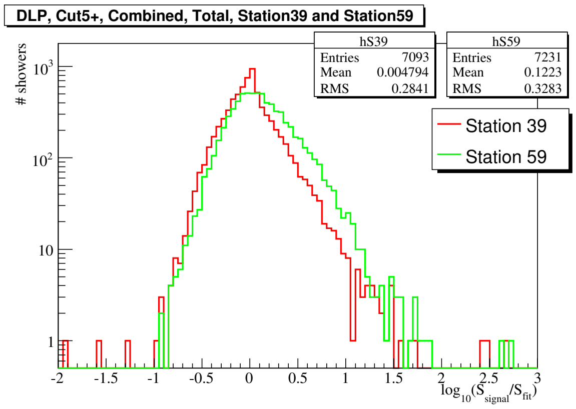

(b)

Figure 18: S_{signal} is the charge produced in a detector, S_{fit} is a signal value determined in the fitting procedure.
(a) Example of a threshold effect on greater distances from a shower core.
(b) Distributions of signals for two differently located stations resulting from (a) behaviour.

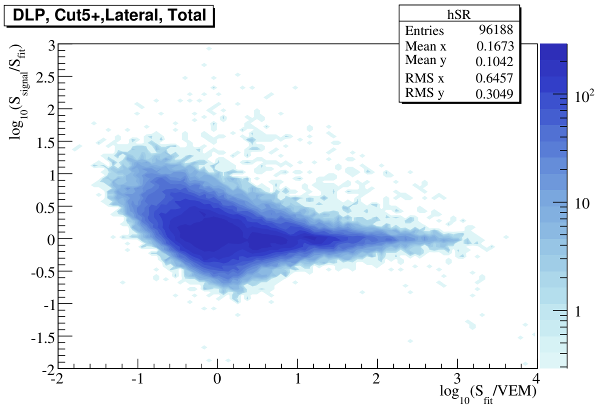

Figure 19: The effect from Fig.18a plotted vs strength of the signal. For big signals $\log_{10}(S_{signal}/S_{fit})$ values fluctuate around zero. Small S_{signal} signals (on the left) are ignored by detectors, so the ratio S_{signal}/S_{fit} increases.

7 Conclusion

Better methods of estimating core position resolution and angular resolution of shower direction were introduced and new estimates were given. No significant asymmetry in x, y coordinates reassures that the analyses with the use of IceTopA and IceTopB subarrays are valid.

A considerable improvement since last studies in S_R reconstructions was indicated. The choice of S_{100} parameter in the fitting procedures was checked and still seems to be correct. However, according to the calculations the use of S_{125} parameter is suggested.

A systematic error of β parameter in fitting DLP as lateral distribution function was encountered and calculated. An additional cut was proposed to deal with misreconstructed events in present fitting procedures. Throughout the calculations Cut5+ proved to be a reasonable choice.

A few threshold effects were indicated, which may be of interest.

8 Acknowledgements

I would like to thank my supervisors in DESY-Zeuthen, Fabian Kislat and Stefan Klepser, for continuous support and guidance, as well as prof. Hermann Kolanoski for his many comments and suggestions. Additional thanks go to Adam Lucke and the other members of the astroparticle group for their friendly reception. I am grateful to Mr. Hiller and Mrs. Baer for their help and organisation of the programme.

Lastly, I thank all the summerstudents for the time spent together at DESY-Zeuthen, 2007.

References

[1] S. Klepser, Scrutinising shower reconstruction algorithms using the subarrays IceTopA and IceTopB, 2006.

[2] S. Klepser, F. Kislat, H. Kolanoski, P. Niessen, A. Van Overloop for the IceCube Collaboration, Lateral distribution of air shower signals and initial energy spectrum. In *Proc. 30th ICRC*, Mérida, 2007.

[3] S. Klepser, private communication